

Article

# Assessment of Sentinel-2 Satellite Images and Random Forest Classifier for Rainforest Mapping in Gabon

Adam Waśniewski <sup>1,2,\*</sup> , Agata Hościło <sup>2</sup> , Bogdan Zagajewski <sup>1</sup>  and Dieudonné Moukétou-Tarazewicz <sup>1,3</sup>

<sup>1</sup> Chair of Geomatics and Information Systems, Department of Geoinformatics, Cartography and Remote Sensing, University of Warsaw, Faculty of Geography and Regional Studies, Krakowskie Przedmieście 30, 00-927 Warsaw, Poland; bogdan@uw.edu.pl (B.Z.); diket22@hotmail.com (D.M.-T.)

<sup>2</sup> Centre of Applied Geomatics, Institute of Geodesy and Cartography, Modzelewskiego 27, 02-679 Warsaw, Poland; agata.hoscilo@igik.edu.pl

<sup>3</sup> Department of Geographical, Environmental and Marine Sciences, Faculty of Letters and Human Sciences, University Omar Bongo of Libreville, Libreville PO Box 17.043, Gabon

\* Correspondence: adam.wasniewski@igik.edu.pl

Received: 23 July 2020; Accepted: 26 August 2020; Published: 28 August 2020



**Abstract:** This study is focused on the assessment of the potential of Sentinel-2 satellite images and the Random Forest classifier for mapping forest cover and forest types in northwest Gabon. The main goal was to investigate the impact of various spectral bands collected by the Sentinel-2 satellite, normalized difference vegetation index (NDVI) and digital elevation model (DEM), and their combination on the accuracy of the classification of forest cover and forest type. Within the study area, five classes of forest type were delineated: semi-evergreen moist forest, lowland forest, freshwater swamp forest, mangroves, and disturbed natural forest. The classification was performed using the Random Forest (RF) classifier. The overall accuracy for the forest cover ranged between 92.6% and 98.5%, whereas for forest type, the accuracy was 83.4 to 97.4%. The highest accuracy for forest cover and forest type classifications were obtained using a combination of spectral bands at spatial resolutions of 10 m and 20 m and DEM. In both cases, the use of the NDVI did not increase the classification accuracy. The DEM was shown to be the most important variable in distinguishing the forest type. Among the Sentinel-2 spectral bands, the red-edge followed by the SWIR contributed the most to the accuracy of the forest type classification. Additionally, the Random Forest model for forest cover classification was successfully transferred from one master image to other images. In contrast, the transferability of the forest type model was more complex, because of the heterogeneity of the forest type and environmental conditions across the study area.

**Keywords:** Sentinel-2; random forest; Gabon; forest type; tropical forest; forest cover

## 1. Introduction

Forest resources fulfil many functions and constitute an important element of human life. Accurate information on the status of forest resources and their constant monitoring at local, regional and global scales is crucial for their sustainable management [1]. Information on forest dynamics is essential for deriving an extent and rate of deforestation [2]. In addition, up-to-date forest maps are important for crisis management, rapid mapping of forest lost, or degradation due to natural hazards, e.g., fires, floods, and severe droughts [3]. In many European and North American countries, forest inventory is regularly carried out by ground-based measurement methods or sometimes using remote sensing techniques. The situation is more complex in developing countries, especially those located in the

equatorial zone, or in mountainous areas, where inventory by traditional methods is expensive and difficult to conduct due to the limited access. In these places the use of satellite remote sensing is essential. The development of remote sensing techniques allows effective and more accurate mapping of wooded areas and determining a condition of forests [4]. Maps of the tropical forest type derived based on satellite data at regional scale have been prepared, for example for Tanzania [5], Ghana [6] and Costa Rica [7]. Hojas-Gascon et al. [5] identified different forest cover densities using 23 SPOT-4 images over one Somalia-Masai ecoregion in Tanzania. In the Ankasa Conservation Area in southwestern Ghana, Laurin et al. [6] discriminated tropical forest type and dominant tree species based on hyperspectral and multitemporal Sentinel-2 data. The authors applied Support Vector Machines (SVM) and Maximum Likelihood Classifier (MLC) and achieved an overall accuracy of 92.3% and 90.7%, respectively. A Random Forest (RF) classifier was successfully used by Fagan et al. [7] in the classification of mature forest, secondary forest and tree plantation species in northern part of Costa Rica based on hyperspectral and Landsat images. The RF classifier was also successfully used to map a forest area and forest changes in Paraguay based on a time series of Landsat data (TM, ETM+, and OLI [8]). The authors analysed the period between 1999 and 2016, and achieved the highest accuracy of 93% for the period 2001–2002 and the lowest 85% for the period 2003–2004. Launching the European Sentinel-2 satellites opened a new era in the application of freely available remote sensed data in forestry. Recently, there has been an increase in research publications focused on the use of the Sentinel-2 data. The advantage of the Sentinel-2 data is higher spatial, temporal and spectral resolution compared to the Landsat data. Sentinel-2 offers 13 spectral bands, including three visible and one near infrared band at a 10 m spatial resolution, four bands in red-edge and two bands in the shortwave infrared (SWIR) spectrum at a 20 m spatial resolution, and three bands at 60 m dedicated to atmosphere and clouds. The probability of getting a cloud-free image is higher due to the launching of the twin Sentinel-2 A and B satellites increasing the revisit time to 5 days. Another advantage of this mission is the wide swath of 290 km, which makes it an ideal sensor for forest analyses over a large area at the regional and national scales. A few studies have focused on the use of the Sentinel-2 data for the classification of forest cover and forest type in tropical zones. Noi and Kappas [9] compared three classification methods—RF, k-Nearest Neighbour (kNN), and SVM—for mapping six land cover classes—residential, impervious surface, agriculture, bare land, forest and water—using a single Sentinel-2 image over a small part of Vietnam. The authors achieved a high overall accuracy ranging from 90% to 95% for three classification methods. Multi-temporal Sentinel-2 data was used by Erinjery et al. [10] in southwestern India to classify vegetation types such as dry deciduous forest, rainforest, water, shade plantation, pattern plantation, open plantation and urban areas. They compared the RF and MLC using Sentinel-2 band at 10 m spatial resolution, NDVI index, texture information and DEM. The MLC approach gave a slightly higher overall accuracy of 85.9% compared to RF 83.5%. Furthermore, the multi-temporal Sentinel-2 data and RF classifier were successfully applied to map plantations in tropical forest in Myanmar [11], and to classify forest and agriculture mosaics in tropical landscape in Brazil [12] and mangrove plantations in Senegal [13]. Sothe et al. [14] studied the potential of Sentinel-2 and Landsat-8 images (multi-temporal spectral reflectance, textural metrics and vegetation indices) for mapping the successional forest stages in a subtropical forest in southern Brazil. The authors applied the RF and SVM methods and achieved slightly higher overall accuracy for RF (92.6–97.4%) compared to SVM (91.9–96.5%). They also highlighted a superior performance of Sentinel-2 data compared to Landsat-8 data. A fusion of multi-temporal Landsat-8, Sentinel-2 data and DEM was used to classify ten forest types in Wuhan, China using the RF classifier [15]. The authors achieved an overall accuracy above 82%.

The main aim of this study is to examine the potential of Sentinel-2 data for forest cover and forest type classification in Gabon. Monitoring of the forest status in Gabon is very important due to the high tree cover loss in primary tropical forest, reaching around 17,877 ha over the period 2001–2018 [16]. There is a limited number of studies that focus on mapping forest cover and forest type using remote sensing techniques in Gabon. Duveiller et al. [17] used a time series of Landsat TM and ETM+ to derive

the land cover and forest lost for the period 1990–2000 over the Central Africa including Gabon. However, there is a need to develop more up-to-date and accurate forest cover and type mapping over tropical countries.

Therefore, the main objectives of this study are: (a) to investigate the potential of various spectral bands collected by Sentinel-2 satellite, vegetation index (NDVI), and digital elevation model (DEM) and its combination on the accuracy of the forest cover and forest type classification and (b) to assess the transferability of the classification models.

## 2. Study Area

The study area is situated in north western part of Gabon—the provinces of Estuaire, Moyen Ogooué, the southern fragment of the province of Woleu-Ntem and the northern fragment of the provinces of Ngounié and Ogooué-Maritime (Figure 1).

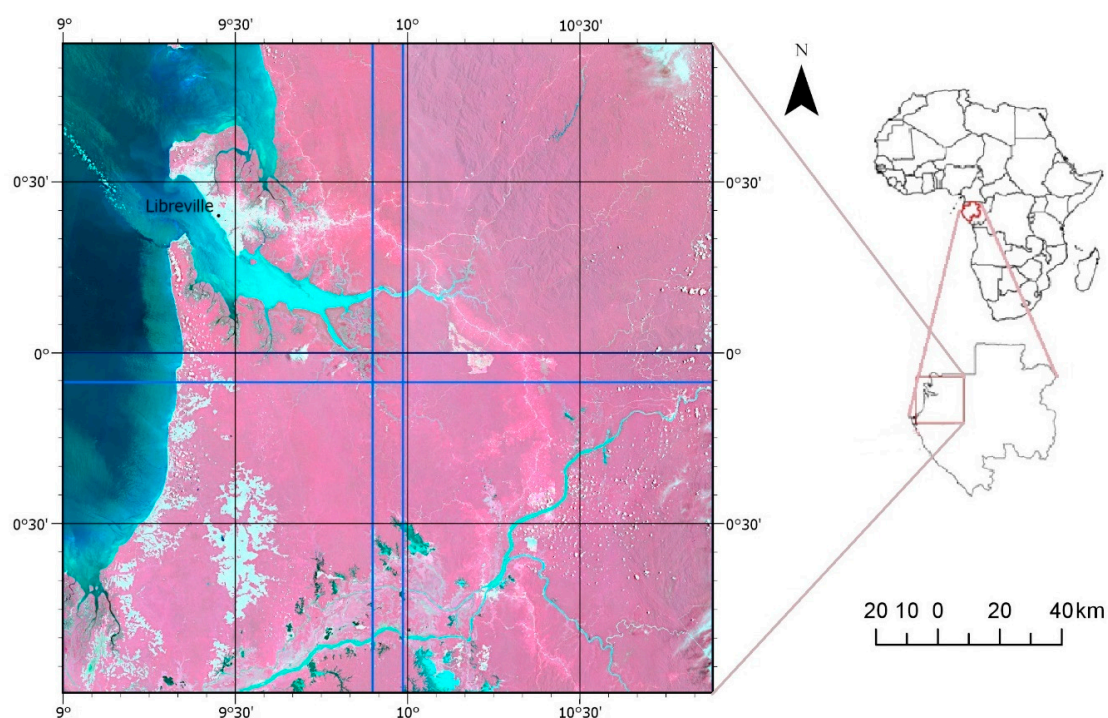


**Figure 1.** Location of the study site; the study area covers the extent of the four Sentinel-2 scenes presented in the colour composite of bands B8, B4 and B3; the blue lines indicate the extent of the Sentinel-2 granules.

The study was conducted over the area of around 40,000 km<sup>2</sup> covering by four Sentinel-2 scenes called granules. The study area is predominantly covered by different forest types: mangroves, freshwater swamp forest, lowland forest, semi-evergreen moist forest disturbed natural forest [18]. The terrain is a combination of the coastal sedimentary plain and the hilly Cristal mountains with the highest peak—The Ndjolé Mounts located 1022 m above sea level (Figure 2). The landscape is cut by large number of rivers.

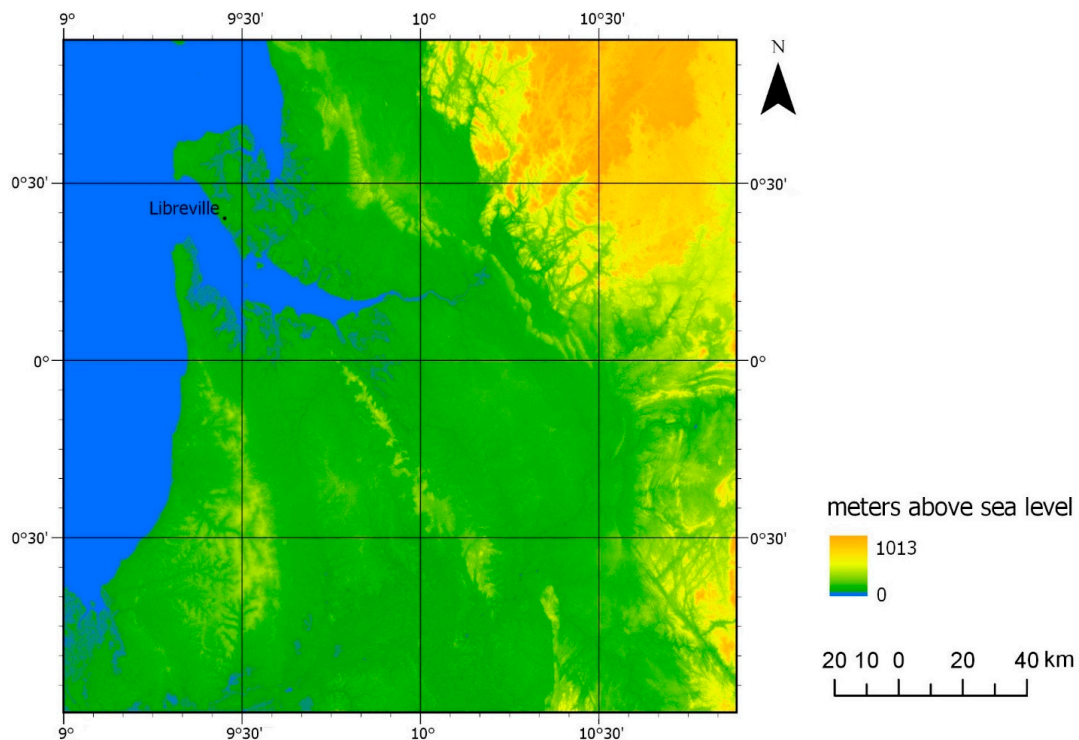


**Figure 2.** Shuttle Radar Topography Mission Digital Elevation Model (SRTM DEM) over the study area.

The climate is hot and humid, as is typical for tropical regions. At Libreville, the capital of Gabon, the average annual rainfall is over 2500 mm. The average annual temperature is 26 °C, in the dry season reaches up to 23 °C and in the rainy season 27 °C [19].

### 3. Data

#### 3.1. Sentinel-2 and DEM

A nearly cloud-free Sentinel-2 image captured on 2 April 2017 was downloaded from the ESA Copernicus Data Hub in the form of four granules, 100 by 100 km. Four adjacent granules forming a 200 by 200 km square were used in this study.

Atmospheric correction was applied to each granule using the Sen2Cor software available within the Sentinel Application Platform (SNAP5.0) provided by ESA [20]. As a result of atmospheric correction, the data was transformed from the Top-Of-Atmosphere value to the Bottom-Of-Atmosphere model (Level-1C to Level-2A). We used the Sentinel-2 bands available at 10 m (blue B2:490 nm, green B3:560 nm, red B4:665 nm, NIR B8:842 nm), and 20 m spatial resolution (red-edge bands: B5:705 nm, B6:740 nm, B7:783 nm, NIR B8a:865 nm, SWIR B11:1610 nm and B12:2190 nm). Bands with 60 m spatial resolution were not used in this study (B1:443 nm, B9:940 nm, B10:1375 nm). All 20 m spatial resolution bands were resampled to a spatial resolution of 10 m using the nearest neighbour resampling method.

The spectral Normalized Difference Vegetation Index (NDVI) was calculated as the difference in red and infrared bands divided by the sum of those bands [21]:

$$\text{NDVI} = (\text{NIR} - \text{RED}) / (\text{NIR} + \text{RED})$$

where NIR refers to B8 (842 nm) and RED refers to B4 (665 nm).

The DEM, used as topographic variable, was derived from the Shuttle Radar Topography Mission (SRTM). SRTM DEM is freely available globally at 1 arc-second at about 30 m spatial resolution. SRTM DEM was obtained from a free satellite viewer of the United States Geological Survey—USGS

Earth Explorer [22]. The SRTM DEM was subset to the study area and resampled to a 10 m spatial resolution using bilinear resampling method.

### 3.2. Reference Datasets

The reference data for forest cover and forest type were obtained from the global land cover maps: GlobCover 2009, and Global Forest Watch. Global Forest Watch is a part of the global forest monitoring program, which offers an interactive map of global forest cover and forest changes (Global Forest Change) developed by the World Resources Institute. Global Forest Watch contains 10 basic land cover classes, including tree cover, primary forest and mangrove forest classes for the year 2015, at a spatial resolution of 30 m. The Global Forest Change database was developed with the initiative of the University of Maryland, based on the analysis of the multi-temporal Landsat images acquired since 2000 [23]. Global Forest Change is a set of digital maps illustrating the extent and direction of changes (loss and gain) over the forest area at the global scale at a spatial resolution of 30 m.

The GlobCover 2009 is a global land cover map developed based on the Envisat MERIS Fine Resolution satellite images with a 300 m spatial resolution acquired over the period December 2004–June 2006. The map consists of 23 land cover classes, including eight forest classes: closed to open (>15%) broadleaved evergreen and/or semi-deciduous forest (>5 m), closed (>40%) broadleaved deciduous forest (>5 m), open (15–40%) broadleaved deciduous forest (>5 m), closed (>40%) needle leaved evergreen forest (>5 m), open (15–40%) needle leaved deciduous or evergreen forest (>5 m), closed to open (>15%) mixed broadleaved and needle leaved forest (>5 m), mosaic forest/shrubland (50–70%)/grassland (20–50%), mosaic grassland (50–70%)/forest/shrubland (20–50%) [24].

## 4. Methods

### 4.1. Selection of Training Samples

To classify forest cover, the selection of the reference sampling plots was performed based on Sentinel-2 images supported by GlobCover 2009 and Global Forest Watch maps. In total, 400 points were randomly distributed over the northwest image, which was chosen as the most representative image in the study area. The points were divided into those located in forest areas and those located in non-forest areas using the visual interpretation. It was assumed that both classes would be represented by 200 forest and 200 non-forest points. In cases of less than 200 points assigned to the class, the missing points were added manually based on the visual interpretation of the satellite images. Selected points were divided into training and verification in the proportion of 50 to 50% (100 training and 100 verification points for each class). The training forest/non-forest points were used to train the classification model over the northwest Sentinel-2 image, and the classification model was then applied to the remaining three images. To assess the accuracy of the classification over the remaining three Sentinel-2 images, the verification points were selected following the same approach like for the northwest image. In total, 100 points representing forest and 100 points representing non-forest areas were chosen for each of the three images.

### 4.2. Identification of Forest Types

The five forest types were identified in the study area: mangroves, freshwater swamp forest, lowland forest, semi-evergreen moist forest and disturbed natural forest. A mangrove forest occurs generally along coasts in or near brackish or salt water, freshwater swamp forest covers waterlogged areas located below 1200 m above sea level. A lowland and semi-evergreen moist forest also occurs below 1200 m above sea level but the lowland forest is characterized by little or no seasonality compared to the evergreen broadleaf and semi-evergreen moist forest, which shows seasonality of flowering and fruiting [18]. A disturbed natural forest refers to the forest disturbed by, for example land clearing, fire, or road construction. The names of the forest type classes followed the definitions of the forest classes developed by the Convention on Biological Biodiversity. The reference samples for

the forest type were identified based on the photointerpretation of Sentinel-2 images supported by analysis of GlobCover 2009, Global Forest Watch and Global Forest Change and local knowledge of the study area. The Global Forest Watch was particularly useful to accurately locate the mangrove forest, while the Global Forest Change database was used to the greatest extent in determining the location of a disturbed natural forest.

For each forest type, between 21 and 24 reference polygons were selected, maintaining the principle of homogeneity of the spectral reflection values within the polygons. The number of pixels in the polygon for each class ranged between 500 and 8000. The size of the polygon and their number varied due to the tonal diversity of pixels (homogeneity) inside of the class and the area represented by each forest type in the image. Reference polygons were divided randomly using a stratified procedure into training and verification in a ratio of 3:7, 30% for training and 70% for verification. The tonal diversity of sampling polygons was analysed during the selection process. The purity of each selected sample was assessed visually by looking at various Sentinel-2 band compositions and by looking at the coefficient of variation (CV) calculated as a ratio of the standard deviation to the mean value calculated for each forest type class for each spectral band. For each forest class in each spectral band, the CV was lower than 20%. A map presenting the location of the reference samples for the forest type is presented in Figure 3.

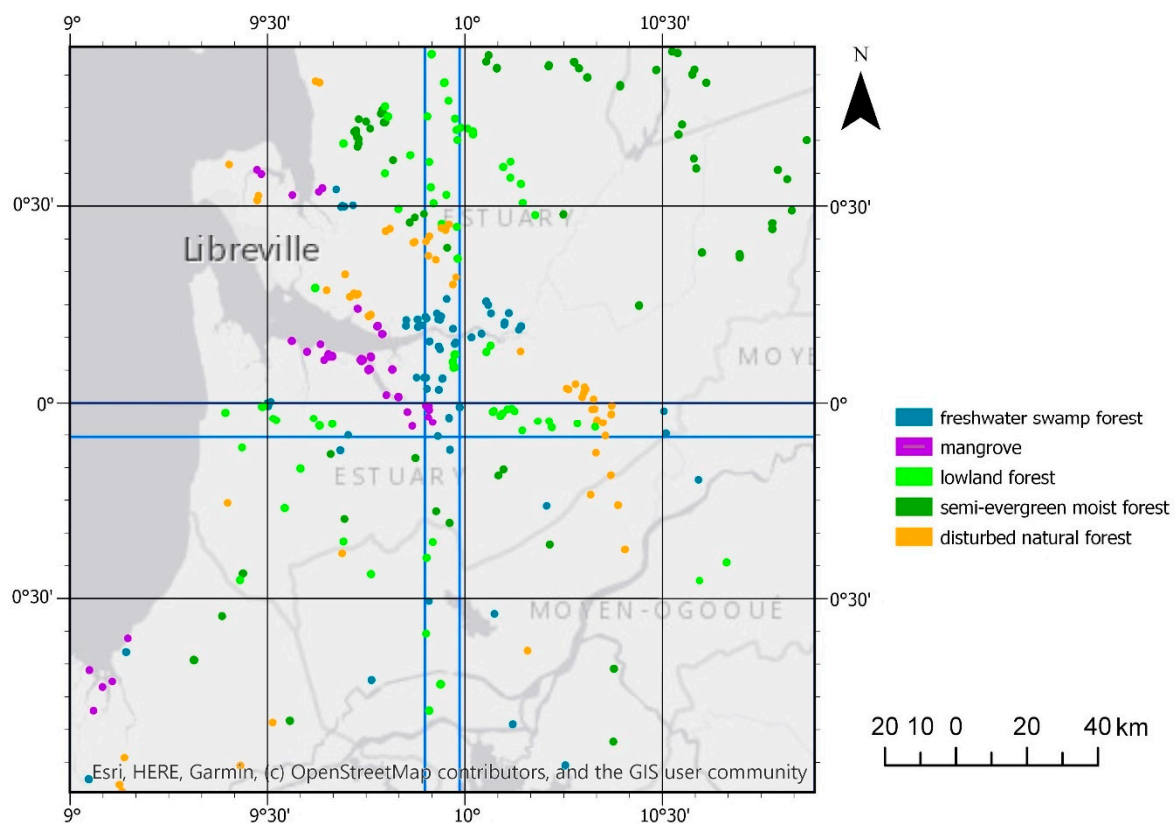


**Figure 3.** Locations of the reference samples for forest type coloured by the forest type classes; the blue lines indicate the extent of the Sentinel-2 granules.

#### 4.3. Classification Method

To determine the importance of individual Sentinel-2 bands and additional datasets, i.e., NDVI and SRTM DEM in the process of classification of forest cover and forest type, the classifications were performed for seven combinations of the input variables:

1. Bands with a spatial resolution of 10 m (4 variables)
2. Bands with a spatial resolution of 10 m and NDVI (5 variables)

3. Bands with a spatial resolution of 10 m and DEM (5 variables)
4. Bands with a spatial resolution of 10 m and 20 m (10 variables)
5. Bands with a spatial resolution of 10 m, 20 m and NDVI (11 variables)
6. Bands with a spatial resolution of 10 m, 20 m and DEM (11 variables)
7. Bands with a spatial resolution of 10 m, 20 m, NDVI and DEM (12 variables)

To perform the classification on a combination of various variables, all 20 m spatial resolution bands and DEM had to be resampled to uniform 10 m spatial resolution. Note, that the resampled 20 m spatial resolution bands are called 20 m spectral bands throughout of the article. The DEM and NDVI were added to the data stack without any additional adjustment.

The classification of forest cover and forest type was performed using a RF classifier [25]. In RF for each of the samples, grow classification by decision tree, with the following modification: at each node, rather than choosing the best split among all predictors, the predictors were randomly sampled, and the best split was chosen from among those variables [26]. A review of the RF applications in remote sensing confirmed that the RF classifier is less sensitive than other streamline machine learning classifiers to the quality of training samples and to overfitting, due to the large number of decision trees produced by randomly selecting a subset of training samples and a subset of variables for splitting at each tree node [27]. The RF classification was carried out using imageRF available at EnMAP-Box 2.0.2, developed at Humboldt-Universität zu Berlin under contract by the Helmholtz Centre, Potsdam—GFZ [28]. A total of 100 decision trees was used for the classification process. The number of selected features was determined by the square root of all features, the Gini Index was used to define the impurity and minimum number of samples in a node was set to one [29,30].

The classification process was divided into two stages. First, the classification of the forest cover was performed. Secondly, the forest type was classified within the forest cover mask.

The classification model for forest cover was trained on the northwest Sentinel-2 image and then the classification model was implemented on the other three images. The forest mask derived at this stage was applied in the forest type classification process. Taking into account the terrain model of the study area, the forest type classification was performed separately for the western and eastern part of the study area. For the western part, the classification model was parameterised using the northwest image, and then the classification model was applied for the southwest image. For the eastern part, the classification model was prepared for the northeast image, and then applied to the southeast image.

The forest cover and forest type classifications were iteratively repeated 84 times, 12 times for each combination of variables, applying out-of-bag data error, which is a method of measuring prediction error of random forests classifier.

#### 4.4. Accuracy Assessment

The accuracy assessment was carried out individually for each classification result using an independent validation dataset. The classification accuracy was expressed as the overall accuracy, kappa coefficient, user's (UA) and producer's (PA) accuracy, and average F1 accuracy value. The F1 value is calculated as a weighted harmonic mean of the UA and PA. The average F1 accuracy represents the arithmetic mean of class wise F1 values. The variation of the F1 values for each classification result is prepared in a form of box plots. The box plot indicates outliers, first quartile, median, third quartile and maximum values. The normalized variable importance was calculated by dividing the raw variable importance by the respective standard deviation [30]. In addition, for the forest type classification the error matrix was calculated.

## 5. Results

### 5.1. Forest Cover Classification

The highest overall accuracy for the forest cover was obtained for the combination of Sentinel-2 bands at 10 m and 20 m spatial resolution and DEM. The median of F1 accuracy value for the most

accurate classification reached 94% (Figure 4) and the overall accuracy ranged between 92.6% for the northeast image and 98.5% for the southwest image (Table 1). The overall accuracy in the northwest image, which was used to train the classifier, was equal to 94.8%. The Kappa coefficient values ranged from 87.1 to 97%. The F1 value of the input variables for the most accurate classification of the forest cover is presented in Figure 4.

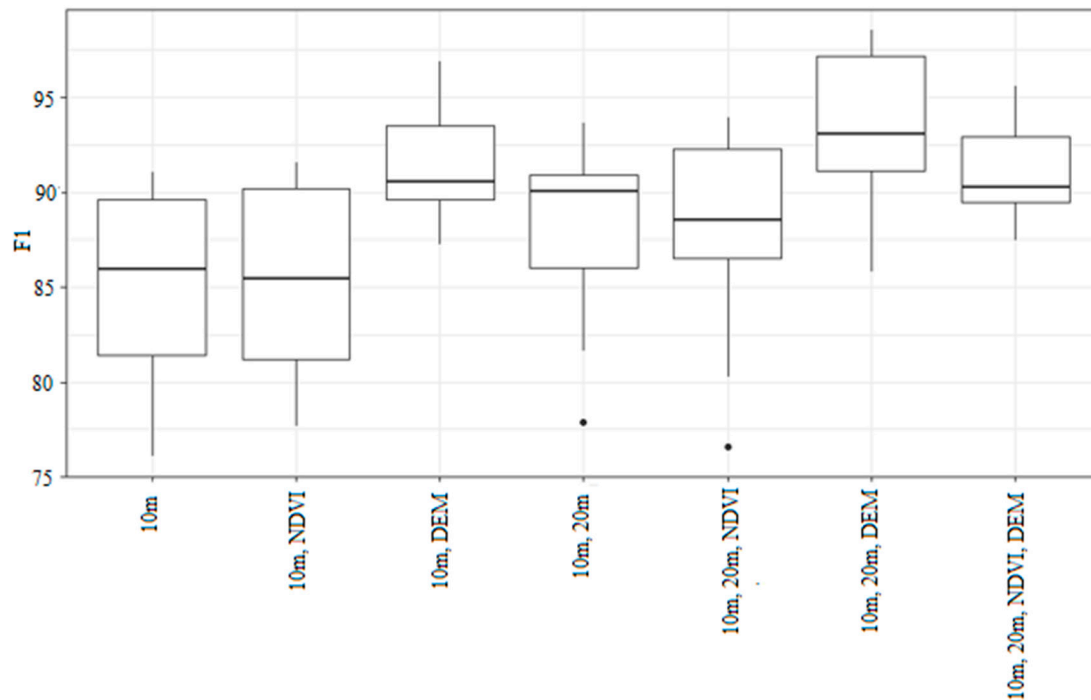


**Figure 4.** Variability of F1 value for the forest cover classification based on the combination of different variables. The box plot indicates outliers, first quartile, median, third quartile and maximum values.

**Table 1.** The accuracy of the forest cover classification based on the combination of Sentinel-2 bands at 10 m and 20 m spatial resolution and DEM, \* indicates image used for the parametrisation of the classification model; UA: user's accuracy, PA: producer's accuracy.

|                   | Northwest Image * | Northeast Image | Southwest Image | Southeast Image |
|-------------------|-------------------|-----------------|-----------------|-----------------|
| Overall accuracy  | 94.8              | 92.6            | 98.5            | 98.0            |
| Kappa coefficient | 89.2              | 87.1            | 97.0            | 96.1            |
| UA/PA Forest      | 89.7/100          | 77.7/92.1       | 96.2/100        | 80.6/98.1       |
| UA/PA Non-forest  | 100/89.7          | 94.5/83.8       | 100/96.1        | 97.5/76.4       |

The second most accurate classification of forest cover was obtained for the combination of 10 m spatial resolution bands and DEM, where the F1 values varied from 87% to 97% and F1 median was equal to 91%. A very similar result was obtained for the combination of bands at 10 m and 20 m, NDVI and DEM, where F1 values ranging from 87% to 95% and F1 median was equal to 90%. The lowest accuracy was achieved for the combination of 10 m spatial resolution bands and the combination of 10 m bands with NDVI, where the median of F1 value was equal to 85% and 86%, respectively. In both cases, the largest value spread (differences of 17 percentage points) was observed.

The analysis of the normalized variable importance for the most accurate classification of the forest cover revealed that the DEM contributed the most to the classification (Figure 5). Among the Sentinel-2 bands, the red-edge B5 (20 m spectral resolution), followed by B2 (10 m) and red-edge B8a (20 m) were the most important variables. Interestingly, B5 showed the smallest spread of variable importance values. The least important were the SWIR bands: B11 and B12, as well as the red-edge B6.

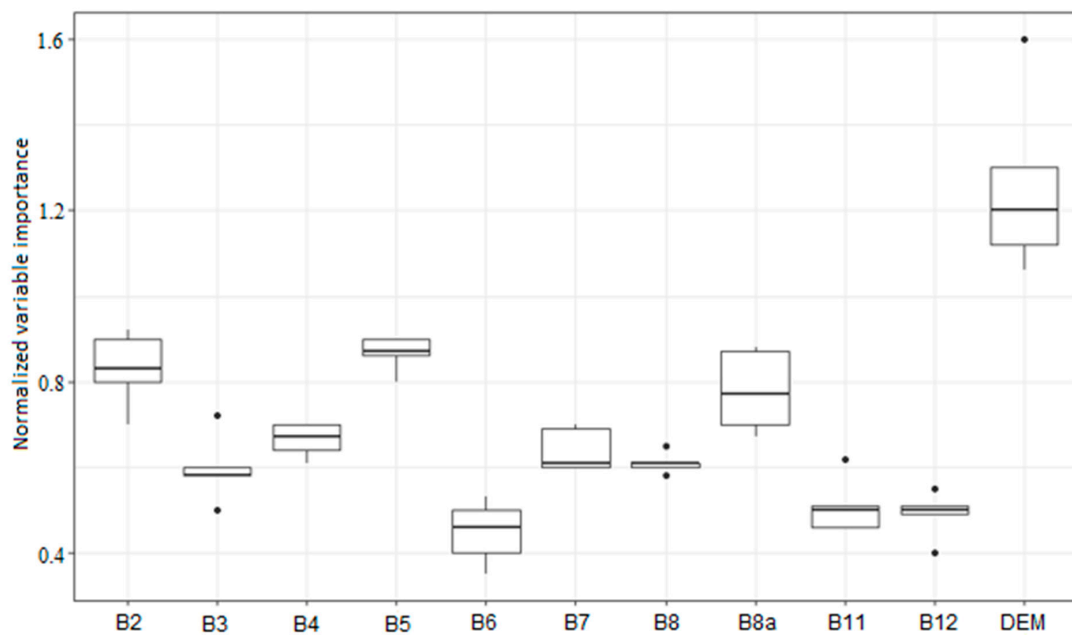


**Figure 5.** Normalized variable importance for the most accurate classification of the forest cover derived using the combination of 10 m (B2, B3, B4, B8), 20 m (B5, B6, B7, B8a, B11, B12) resolution bands and DEM (11 variables).

## 5.2. Forest Type Classification

The highest accuracy of the classification of forest type was obtained for the combination of Sentinel-2 bands at 10 m, 20 m spatial resolution and DEM. For this classification, the overall accuracy ranged from 83.4% for the southeast image to 97.4% for the northwest image (Table 2). The Kappa coefficient values varied from 71.5% to 95.7%, respectively. For the western images, the overall accuracy decreased by around 6 percentage points, compared to the image used to parametrise the classification model. In the case of the eastern images, the difference in the classification accuracy was much larger and reached up to 14 percentage points.

**Table 2.** The accuracy of forest type classification based on the combination of Sentinel-2 bands at 10 and 20 m spatial resolution and DEM, \* images used for parametrisation of the classification models, UA: user's accuracy, PA: producer's accuracy.

|                                   | Northwest<br>Image * | Southwest<br>Image | Northeast<br>Image * | Southeast<br>Image |
|-----------------------------------|----------------------|--------------------|----------------------|--------------------|
| Overall accuracy                  | 95.9                 | 90.1               | 97.4                 | 83.4               |
| Kappa coefficient                 | 93.1                 | 85.3               | 95.7                 | 71.5               |
| UA/PA Disturbed natural forest    | 61.5/71.4            | 66.4/80.4          | 100/98.0             | 93.4/84.8          |
| UA/PA Freshwater swamp forest     | 60.3/100             | 84.8/91.1          | 89.4/100             | 100/64.9           |
| UA/PA Lowland forest              | 96.9/94.5            | 93.6/97.6          | 99.4/93.5            | 76.3/97.9          |
| UA/PA Semi-evergreen moist forest | 99.9/86.9            | 97.5/77.2          | 100/100              | 96.0/67.1          |
| UA/PA Mangroves                   | 99.9/100             | 96.7/79.9          | NA                   | NA                 |

Figure 6 presents the F1 values for classification of forest type using seven combinations of input variables. The F1 median value for the most accurate classification that was obtained using a combination of the 10 m and 20 m bands and DEM reached up to 88% and the F1 value ranged from 78 to 96%.

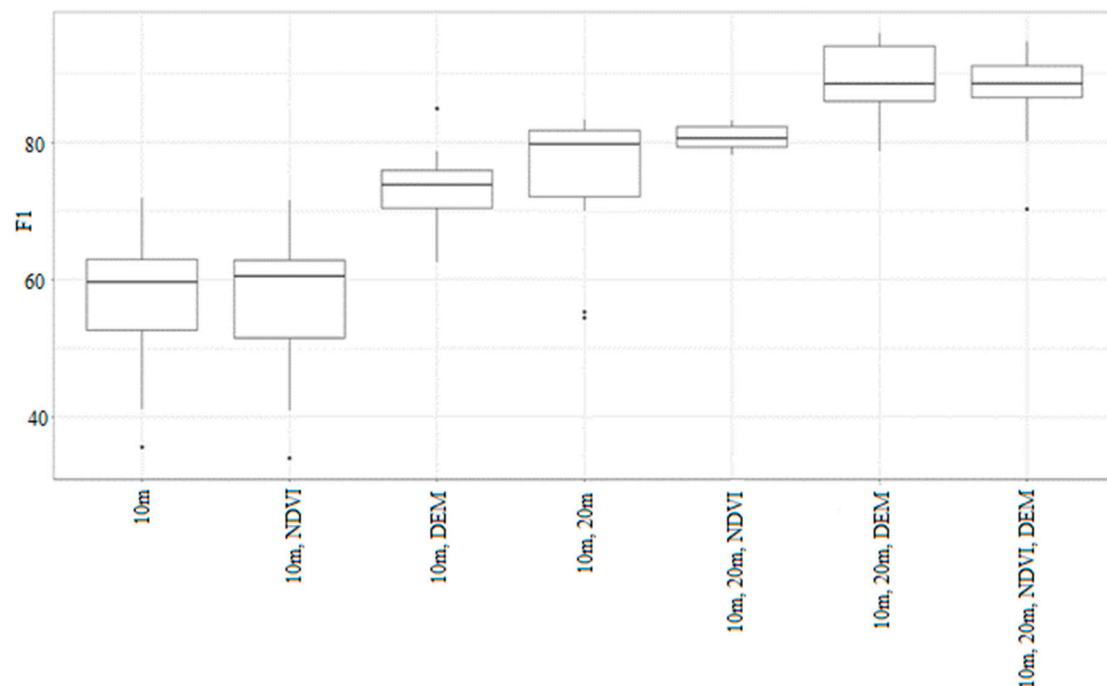


**Figure 6.** The F1 value for the forest type classification based on the combination of different variables.

The second most accurate classification result was obtained using the combination of Sentinel-2 bands at 10 m and 20 m spatial resolution, NDVI and DEM. Here, the median F1 value was also equal to 88%, but the maximum F1 value was lower compared to the previous case. The combination of all spectral bands and NDVI reached the median F1 accuracy values slightly above 80%. Similar results were obtained for the combination of Sentinel-2 bands at 10 m and 20 m. In this case, the F1 value spread was much larger compared to the combination with NDVI. The lowest F1 value, equal to around 60%, was obtained for the classification performed based on the combination of four 10 m spatial resolution bands and 10 m bands combined with NDVI. The largest variation in the F1 values was observed for the four 10 m bands, as well as for the combination of 10 m and NDVI.

The map of the most accurate classification of forest type derived based on the combination of 10 m, 20 m spatial resolution bands and DEM is presented in Figure 7.

The normalised variable importance for the most accurate forest type classification derived based on the combination of 10 m, 20 m Sentinel-2 bands and DEM is presented in Figure 8. Among the various input variables, the DEM appeared to be the most important variable in distinguishing the forest type.

Among the Sentinel-2 spectral bands, the red-edge B5 and B6 followed by the SWIR B12 contributed the most to the accuracy of the forest type classification. Interestingly, the 10 m spectral bands—B2, B3, B4 and B8—were the least useful in the classification of forest type. The SWIR B11 was shown to have the highest spread of the normalised variable importance values.

Forest type classification error matrixes for four Sentinel-2 images were combined into a summary table, with the percentage of correctly classified pixels of each forest type being presented in Table 3.

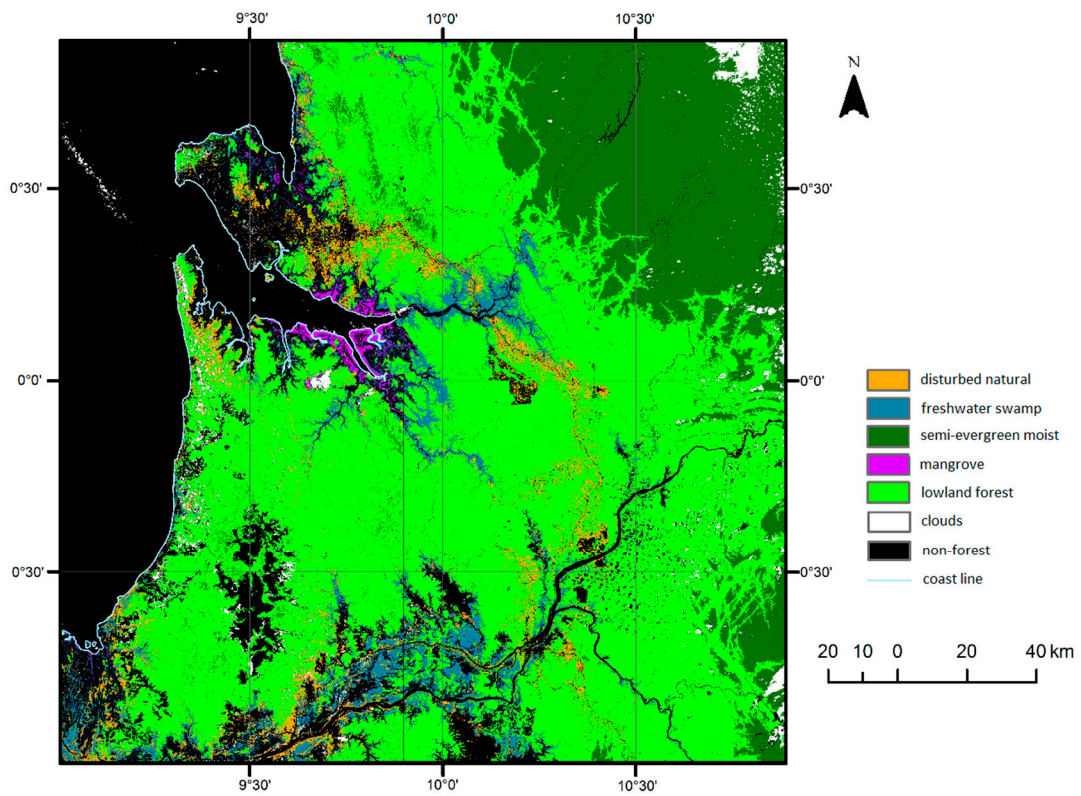


**Figure 7.** Forest type map obtained as a result of RF classification based on the combination of 10 m, 20 m Sentinel-2 bands and DEM.

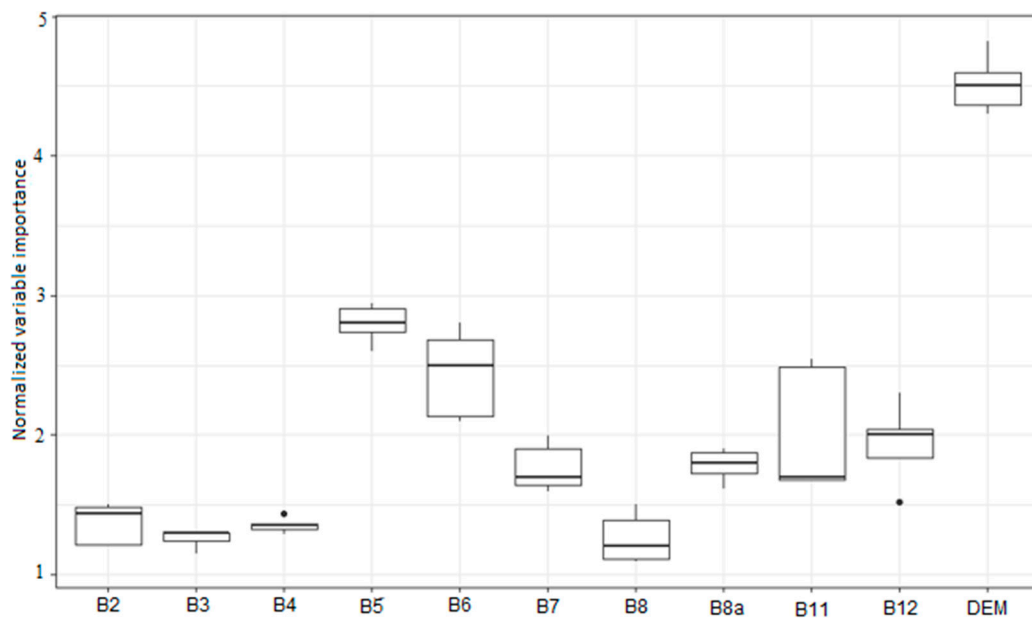


**Figure 8.** Normalized variable importance for the best classification of forest type derived using a combination of 10 m (B2, B3, B4, B8), 20 m (B5, B6, B7, B8a, B11, B12) resolution bands and DEM (11 variables).

**Table 3.** Error matrix for RF classification of forest type for the most accurate classification result.

|                             | Disturbed<br>Natural Forest | Freshwater<br>Swamp Forest | Semi-Evergreen<br>Moist Forest | Mangroves | Lowland<br>Forest |
|-----------------------------|-----------------------------|----------------------------|--------------------------------|-----------|-------------------|
| Disturbed natural forest    | 85%                         | 2%                         | 0%                             | 1%        | 1%                |
| Freshwater swamp forest     | 4%                          | 84%                        | 0%                             | 1%        | 2%                |
| Semi-evergreen moist forest | 2%                          | 0%                         | 82%                            | 0%        | 1%                |
| Mangroves                   | 0%                          | 0%                         | 0%                             | 98%       | 0%                |
| Lowland forest              | 9%                          | 14%                        | 18%                            | 0%        | 96%               |

Mangrove forest was classified the most accurately, with up to 98% of pixels correctly classified. The second most well-classified forest type was lowland forest, with 96% correctly classified pixels, with only 1–2% being incorrectly classified as disturbed natural forest, freshwater swamp forest and semi-evergreen moist forest. A similar percentage of correctly located pixels was achieved for the disturbed natural forest (85%) and freshwater swamp forest (84%). The disturbed natural forest and freshwater swamp forest mixed to the greatest extent with the lowland evergreen forest, with 9% and 14% pixels, respectively. The lowest accuracy was obtained for the evergreen humid forest—82%. This type of forest was mixed only with the lowland forest, and 18% of the pixels were incorrectly classified as semi-evergreen moist forest.

## 6. Discussion

This study presented the potential of Sentinel-2 bands and its combination with NDVI and DEM in the classification of forest cover and type in the tropical forest in Gabon. The accuracy of the classification results obtained in this study is comparable to or more accurate than the results presented by other studies. The accuracy of the forest cover classification is in line with the studies by Noi and Kappas [9] and Sothe et al. [14]. Both authors applied the RF approach to Sentinel-2 data to map the forest cover in Vietnam and southern Brazil, respectively. Sothe et al., 2017 obtained an overall accuracy of 92.6–97.4%, which is comparable to our results. By contrast, Noi and Kappas [9] achieved a lower accuracy of 83.5% [10]. Atsri et al. [29] mapped the forest cover in Togo applying the highest probability algorithm to single images from Sentinel-2, Landsat TM and ETM+ data and achieved an overall accuracy of 93% for Sentinel-2 data, which is slightly lower than that presented in this study. The comparison of the results of the forest cover classification using Landsat and Sentinel-2 data revealed higher accuracy for the Sentinel-2 data, which may be related to the higher spatial resolution of this data. For example, Duveiller et al. [17] obtained a slightly lower accuracy (93%) for classification of the forest cover in Central Africa based on Landsat TM and ETM+ images for the period 1990–2000 using the unsupervised object classification. Studies by Da Ponta et al. [8] and Silveira et al. [31] focused on the tropical forest classification using the RF approach and a time series of Landsat images (1999–2016) in Paraguay and (2003–2016) in Brazil, respectively, and presented less accurate results than those achieved in our study based on Sentinel-2 data. In the study in Paraguay, the overall accuracy ranged from 85% to 93% (classification was carried out for individual years), whereas in Brazil, it ranged from 63% to 96%, depending on different geostatistical features used in RF classification.

Our results are in line with the results of other studies on forest types in tropical zones. Connette et al. [30] applied the RF algorithm to Landsat-8 data to classify four forest types (upland evergreen, lowland evergreen, mixed deciduous and mangrove forest) in Myanmar and obtained a much lower user's and producer's accuracy of 79%. They achieved however similar lowest accuracy results for degraded forest, with 24% of reference points being misclassified. In our study, disturbed forest also had the lowest accuracy in the northwest Sentinel-2 image (UA = 61% and PA = 71%). Another similarity concerns the high accuracy of mangrove forest, with Connette et al. [30] reaching 95% UA and 84% PA, while we achieved the UA of 96–99% and PA of 79–100%. Fagan et al. [7] tested the RF classifier for mapping land cover, including the forest type classes mature forest, secondary forest, and tree plantation, in the northern part of Costa Rica. The authors applied

classification models to the hyperspectral and Landsat data and achieved a producer's accuracy of 83–88%, depending on the different variables used in classification model.

In another study in the Virgin Islands, Kennaway et al. [32] obtained a lower overall accuracy (72%) using the decision tree method for forest type mapping based on Landsat ETM+, DEM and LiDAR data compared to our results, where the overall accuracy reached 83–98%. Comparing the classification accuracy for the forest type mapping using the Sentinel-2 data, our results are in line with the results obtained by Laurin et al. [6]. The authors mapped two forest types (evergreen and moist semi-deciduous forest) in south Ghana applying the SVM method to Sentinel-2 and hyperspectral data and achieved an overall accuracy of 92%. A study by Saini et al. [33] demonstrated the superiority of the Sentinel-2 data over the Landsat-8 data in vegetation type classification in India. They tested both datasets for mapping vegetation types including wheat, fodder, trees, fallow land sugarcane, water, other crops built up and sandy area using the RF approach. The overall accuracy achieved for Sentinel-2 10 m spatial bands was higher by 1.7 percentage points (88.4%) than that achieved by Landsat-8 (86.7%); using 20 m Sentinel-2 bands, the overall accuracy increased by 3.4 percentage point (90.1%) relative to Landsat-8 bands.

The analysis of the variable importance for the accuracy of the classification results made it possible to examine the usefulness of various Sentinel-2 spectral bands, NDVI and DEM and its combination in the classification of forest cover and types. The obtained results confirmed the potential of the combination of 10 m and 20 m spatial resolution bands in the classification of forest cover. By adding the 20 m bands, the accuracy of the classification for both the forest cover and forest type improved significantly. The median of F1 value for forest cover, derived using a combination of only 10 m bands, was 4 percentage points lower than applying the combination of 10 m and 20 m spectral bands: 85.9% and 91%, respectively. The use of the combination of 10 m and 20 m spectral bands in the classification of forest type resulted in a significant increase of the median F1 value (F1 = 79%) compared to the 10 m bands alone (F1 = 59%). Further increase in the classification accuracy was observed after adding the DEM. By adding the DEM to the combination of 10 m spectral bands, the overall accuracy increased by 14 percentage points, reaching 73%. Furthermore, adding DEM to the combination of 10 m and 20 m spectral bands caused an increase in median F1 value from 79% to 88%, respectively. The DEM was demonstrated to be particularly important in classifying semi-evergreen moist forest in mountain areas, which occurs at the highest altitudes in the northeast Sentinel-2 image. The presence of this forest is highly dependent on elevation, which may explain the high importance of DEM in the classification of this forest type. Classification results and analysis of the validity of variables confirmed that the DEM is more important in the separation of the forest type than in forest cover. The importance of the DEM for the classification of forest type has been highlighted by several researchers. Connette et al. [34] found that the quality and accuracy of classification is influenced by DEM, which provides information about height above sea level and allows more precise pixel allocation to appropriate forest types. This research was conducted to investigate the use of multi-spectral Landsat-8 imagery for mapping mangrove, lowland evergreen, upland evergreen and mixed deciduous forest in Myanmar. Dorren et al. [35] confirmed the importance of DEM as an additional variable in Landsat data for the classification of forest type by MLC in steep mountain areas in Austria; by adding the DEM, the classification result was improved from 64 to 73%. A recent study by Hoscilo and Lewandowska [36] also showed the DEM to be the most important variable in the separation of forest type by RF classifier using multi-temporal Sentinel-2 data in temperate mountain forest. The potential of DEM was also demonstrated in forest type mapping over the China mountain area, where by adding the DEM to Landsat-8 and Sentinel-2 data, the overall accuracy increased by 15.2 percentage points to 82.8% [15]. These findings confirm that DEM is particularly important in the classification of the forest types in high-altitude areas.

By contrast, adding the NDVI index to the combination of 10 m bands caused a slight increase in F1 from 0.2 to 0.5 percentage points. However, the NDVI added to the combination of 10 m and 20 m bands decreased the median F1 value by 1 percentage point. Interestingly, adding NDVI to the combination of 10 m, 20 m and DEM resulted in a deterioration of the accuracy by 3 percentage points.

The low importance of the NDVI has been reported by other researchers for tree species classification in New Caledonia [37] and the mapping of tropical forest changes in Brazil [31].

The red-edge bands, in particularly B5 and B6, were shown to be more important in the classification of forest type than in forest cover. Interestingly, B6 was much less important for the classification of the forest area compared to B5. Red-edge is less sensitive to atmospheric effects and soil, and so it can provide information not available from a combination of near infrared and visible spectral bands. Additionally, reflectance around red-edge is more sensitive to chlorophyll and nitrogen content, LAI, and biomass [38]. The usefulness of the red-edge bands in the forest type classification has been highlighted by other studies: Wessel et al. [39] found that B6 had a significant impact on the accuracy of forest classification and that the red-edge showed clearly visible differences in spectral profile. The importance of the red-edge band was also observed by Immitzer et al. [40] in the classification of tree species in Austria. The least informative for the classification of forest type were the visual spectral bands, B2, B3, B4 and NIR B8, available at the 10 m spatial resolution. By contrast, the red-edge B6 and SWIR B11 and B12 were shown to be less important in the classification of forest cover.

The accuracy assessment for the classification of forest cover performed on the independent verification dataset revealed that the model trained on one representative image could be successfully transferred and applied to other images that are characterised by a comparable landscape and the same forest classes. The transferability of the forest type model was more complex than the forest cover model. This is due to the heterogeneity of the forest types and the environmental condition across the study area. The mangrove forest occurred only in the western part of the study area. Therefore, it was necessary to develop two separate forest type classification models, one for the western part along the shoreline, and a second for the eastern part of the study area. The results of the forest type classification confirmed the higher accuracy for the images used to train the model. Firstly, the RF model was trained on the northwest image and applied on the southwest image, obtaining higher accuracy on the trained image (95%) compared to the image where the model was reused (90%). Secondly, the RF model was trained on the northeast image and applied on the southeast image. Here, the difference in accuracy was larger, and decreased from 97% to 83%. This confirms the complexity of the model transferability for the forest type classification. The limitations associated with transferring the classification models were also observed during the monitoring of woody cover in tropical dry forest in Tanzania and Ethiopia by Van Passel et al. [41]. The authors concluded that the classification accuracy is better on image used to train the model than by reusing this model on different images. They stressed that the models trained in a more heterogeneous landscape were expected to be more accurate, which was also demonstrated in our study.

The high temporal resolution of the Sentinel-2 data is of great advantage for forest monitoring and management; however, in the tropics, the high degree of cloud cover is the most obvious constraint for obtaining cloud-free coverage. The solution could be the use of radar data or the synergy of optical and radar data allowing the analysis of the Earth's surface regardless of the time of day and cloudiness. For example, Reiche et al. [42] used the Sentinel-1 radar and optical MODIS data to determine tropical forest cover loss in Indonesia, and achieved producer's and user's accuracy of 95%. Radar data has also been used for tropical forest disturbance mapping in Peru and Gabon [43]. The authors combined a time series of optical Landsat-8, Sentinel-2 with radar Sentinel-1, and mapped non-forest, undisturbed forest and disturbed forest, obtaining an overall accuracy of 93% for Peru and 98% for Gabon.

## 7. Conclusions

This study investigated the potential of various spectral Sentinel-2 bands and their combination with NDVI and DEM for mapping forest cover and forest type in Gabon.

- The highest accuracy for the classification of forest cover and forest type was obtained for the combination of Sentinel-2 bands at 10 m, 20 m spatial resolution and DEM.
- By adding the 20 m bands to the 10 m bands, the accuracy of the classification for both the forest cover and forest type improved significantly.

- The use of the NDVI did not increase the accuracy of the forest cover and type classifications.
- DEM was demonstrated to be the most important variable in the classification of forest type.
- Among the Sentinel-2 spectral bands, the red-edge B5 and B6, followed by the SWIR B12, contributed the most to the accuracy of the forest type classification. Interestingly, the 10 m spectral bands, B2, B3, B4 and B8, were the least useful in the classification of forest type.
- The mangrove forest was classified with a high accuracy of 98%, followed by lowland forest (96%), disturbed natural forest (85%) and freshwater swamp forest (84%).
- The RF model for forest cover classification was successfully transferred from one master image to other images. In contrast, the transferability of the forest type model was more complex, because of the heterogeneity of the forest types and environmental conditions across the study area.
- The accuracy of the forest type classification was higher for the image used to train the model compared to the image where the model was reused.
- The forest cover and forest type classification models can be successfully reused on other images if the same land cover classes occur in both images.

**Author Contributions:** Conceptualization, methodology: A.W., A.H., B.Z.; validation, formal analysis, investigation, resources and data curation: A.W.; local knowledge of the study area: D.M.-T.; all authors prepared the manuscript. Supervision, project administration and funding acquisition: A.H. and B.Z. All authors have read and agreed to the published version of the manuscript.

**Funding:** The publishing costs were covered by the Polish Ministry of Science and Higher Education, project the theme No. 500-D119-12-1190000.

**Acknowledgments:** We are grateful to the editors and the anonymous reviewers for their constructive comments and suggestions that helped to improve this manuscript.

**Conflicts of Interest:** The authors declare no conflict of interest.

## References

1. Koppad, A.G.; Janagoudar, B.S. Vegetation analysis and land use land cover classification of forest in Uttara Kannada district India using remote sensing and GIS techniques. *ISPRS Int. Arch. Photogramm. Remote Sens. Spat. Inf. Sci.* **2017**, *42*, 121–125. [[CrossRef](#)]
2. Rahman, M.M.; Sumantyo, J.T.S. Mapping tropical forest cover and deforestation using synthetic aperture radar (SAR) images. *Appl. Geomat.* **2010**, *2*, 113–121. [[CrossRef](#)]
3. McRoberts, R.E.; Tomppo, E.O. Remote sensing support for national forest inventories. *Remote Sens. Environ.* **2007**, *110*, 412–419. [[CrossRef](#)]
4. Wang, Z.B.; Andrew. An integrated method for forest canopy cover mapping using Landsat ETM+ imagery. In Proceedings of the ASPERS/MAPRS2009 Fall Conference, San Antonio, TX, USA, 16–19 November 2009; pp. 16–19.
5. Hojas-Gascon, L.; Belward, A.; Eva, H.; Ceccherini, G.; Hagolle, O.; Garcia, J.; Cerutti, P. Potential improvement for forest cover and forest degradation mapping with the forthcoming sentinel-2 program. *ISPRS Int. Arch. Photogramm. Remote Sens. Spat. Inf. Sci.* **2015**, *40*, 417–423. [[CrossRef](#)]
6. Laurin, G.V.; Puletti, N.; Hawthorne, W.; Liesenberg, V.; Corona, P.; Papale, D.; Chen, Q.; Valentini, R. Discrimination of tropical forest types, dominant species, and mapping of functional guilds by hyperspectral and simulated multispectral Sentinel-2 data. *Remote Sens. Environ.* **2016**, *176*, 163–176. [[CrossRef](#)]
7. Fagan, M.E.; DeFries, R.S.; Sesnie, S.E.; Arroyo-Mora, J.P.; Soto, C.; Singh, A.; Townsend, P.A.; Chazdon, R.L. Mapping species composition of forests and tree plantations in northeastern Costa Rica with an integration of hyperspectral and multitemporal landsat imagery. *Remote Sens.* **2015**, *7*, 5660–5696. [[CrossRef](#)]
8. Da Ponte, E.; Mack, B.; Wohlfart, C.; Rodas, O.; Fleckenstein, M.; Oppelt, N.; Dech, S.; Kuenzer, C. Assessing forest cover dynamics and forest perception in the Atlantic forest of Paraguay, combining remote sensing and household level data. *Forests* **2017**, *8*, 389. [[CrossRef](#)]
9. Noi, P.T.; Kappas, M. Comparison of random forest, k-nearest neighbor, and support vector machine classifiers for land cover classification using sentinel-2 imagery. *Sensors* **2018**, *18*, 18. [[CrossRef](#)]

10. Erinjery, J.J.; Singh, M.; Kent, R. Mapping and assessment of vegetation types in the tropical rainforests of the Western Ghats using multispectral Sentinel-2 and SAR Sentinel-1 satellite imagery. *Remote Sens Environ.* **2018**, *216*, 345–354. [[CrossRef](#)]
11. Nomura, K.; Mitchard, E.T.A. More than meets the eye: Using sentinel-2 to map small plantations in complex forest landscapes. *Remote Sens.* **2018**, *10*, 1693. [[CrossRef](#)]
12. Mercier, A.; Betbeder, J.; Rumiano, F.; Baudry, J.; Gond, V.; Blanc, L.; Bourgoïn, C.; Cornu, G.; Ciudad, C.; Marchamalo, M.; et al. Evaluation of sentinel-1 and 2 time series for land cover classification of forest-agriculture mosaics in temperate and tropical landscapes. *Remote Sens.* **2019**, *11*, 979. [[CrossRef](#)]
13. Navarro, J.A.; Algeet, N.; Fernandez-Landa, A.; Esteban, J.; Rodriguez-Noriega, P.; Guillen-Climent, M.L. Integration of UAV, sentinel-1, and sentinel-2 data for mangrove plantation aboveground biomass monitoring in Senegal. *Remote Sens.* **2019**, *11*, 77. [[CrossRef](#)]
14. Sothe, C.; de Almeida, C.M.; Liesenberg, V.; Liesenberg, V. Evaluating sentinel-2 and landsat-8 data to map successional forest stages in a subtropical forest in southern Brazil. *Remote Sens.* **2017**, *9*, 838. [[CrossRef](#)]
15. Liu, Y.A.; Gong, W.S.; Hu, X.Y.; Gong, J.Y. Forest type identification with random forest using sentinel-1A, sentinel-2A, multi-temporal landsat-8 and DEM data. *Remote Sens.* **2018**, *10*, 946. [[CrossRef](#)]
16. Butler, R.A. Deforestation Statistics for Gabon. Mongabay. 2018. Available online: <https://rainforests.mongabay.com/deforestation/archive/Gabon.htm> (accessed on 24 June 2020).
17. Duveiller, G.; Defourny, P.; Desclee, B.; Mayaux, P. Deforestation in Central Africa: Estimates at regional, national and landscape levels by advanced processing of systematically-distributed Landsat extracts. *Remote Sens. Environ.* **2008**, *112*, 1969–1981. [[CrossRef](#)]
18. Montreal, C. Convention on Biological Diversity. Definitions. 2014. Available online: <https://www.cbd.int/forest/definitions.shtml> (accessed on 24 June 2020).
19. Climate—Gabon. Climates to Travel. World Climate Guide. Available online: <https://www.climatestotravel.com/climate/gabon> (accessed on 24 June 2020).
20. Sen2Cor. Science Toolbox Exploitation Platform (STEP). European Space Agency. Available online: <http://step.esa.int/main/third-party-plugins-2/sen2cor/> (accessed on 7 July 2017).
21. Rouse, J.W.; Haas, R.H.; Scheel, J.A.; Deering, D.W. Monitoring vegetation systems in the great plains with ERTS. In Proceedings of the 3rd Earth Resource Technology Satellite (ERTS) Symposium NASA, Washington, DC, USA, 10–14 December 1973; pp. 309–317, document ID:19740022614.
22. U.S. Geological Survey. EarthExplorer—Home. Available online: <https://earthexplorer.usgs.gov/> (accessed on 7 July 2017).
23. Hansen, M.C.; Potapov, P.V.; Moore, R.; Hancher, M.; Turubanova, S.A.; Tyukavina, A.; Thau, D.; Stehman, S.V.; Goetz, S.J.; Loveland, T.R.; et al. High-resolution global maps of 21st-century forest cover change. *Science* **2013**, *342*, 850–853. [[CrossRef](#)]
24. Bontemps, S.; Defourny, P.; Van Bogaert, E.; Arino, O.; Kalogirou, V.; Perez, J.R. GLOBCOVER 2009 Products description and validation report. *ESA Bull.* **2011**, *53*. [[CrossRef](#)]
25. Breiman, L. Random forests—Random features. *Mach. Learn.* **2001**, *45*, 5–32. [[CrossRef](#)]
26. Liaw, A.; Wiener, M. Classification and regression by randomForest. *R News* **2002**, *2*, 18–22.
27. Belgiu, M.; Dragut, L. Random forest in remote sensing: A review of applications and future directions. *ISPRS J. Photogramm. Remote Sens.* **2016**, *114*, 24–31. [[CrossRef](#)]
28. Van der Linden, S.; Rabe, A.; Held, M.; Jakimow, B.; Leitão, P.J.; Okujeni, A.; Schwieder, M.; Suess, S.; Hostert, P. The EnMAP-Box-A toolbox and application programming interface for EnMAP data Processing. *Remote Sens.* **2015**, *7*, 11249–11266. [[CrossRef](#)]
29. Waske, B.; Van Der Linden, S.; Oldenburg, C.; Jakimow, B.; Rabe, A.; Hostert, P. imageRFa user-oriented implementation for remote sensing image analysis with Random Forests. *Environ. Model. Softw.* **2012**, *35*, 192–193. [[CrossRef](#)]
30. Jakimow, B.; Oldenburg, C.; Rabe, A.; Waske, B.; Van Der Linden, S.; Hostert, P. *Manual for Application: Imagerf (1.1)*; Universität Bonn, Institute of Geodesy and Geo Information, Department of Photogrammetry and Humboldt-Universität zu Berlin, Geomatics Lab.: Berlin, Germany, 2012.
31. Silveira, E.M.O.; Bueno, I.T.; Acerbi, F.W.; Mello, J.M.; Scolforo, J.R.S.; Wulder, M.A. Using spatial features to reduce the impact of seasonality for detecting tropical forest changes from landsat time series. *Remote Sens.* **2018**, *10*, 808. [[CrossRef](#)]

32. Kennaway, T.A.; Helmer, E.H.; Lefsky, M.A.; Brandeis, T.A.; Sherrill, K.R. Mapping land cover and estimating forest structure using satellite imagery and coarse resolution lidar in the Virgin Islands. *J. Appl. Remote Sens.* **2008**, *2*, 023551. [[CrossRef](#)]
33. Saini, R.; Ghosh, S. Exploring capability of Sentinel-2 for vegetation mapping using Random Forest. *ISPRS Int. Arch. Photogramm. Remote Sens. Spat. Inf. Sci.* **2018**, *42*, 1499–1502. [[CrossRef](#)]
34. Connette, G.; Oswald, P.; Songer, M.; Leimgruber, P. Mapping distinct forest types improves overall forest identification based on multi-spectral landsat imagery for myanmar's Tanintharyi region. *Remote Sens.* **2016**, *8*, 882. [[CrossRef](#)]
35. Dorren, L.K.A.; Maier, B.; Seijmonsbergen, A.C. Improved landsat-based forest mapping in steep mountainous terrain using object-based classification. *For. Ecol.* **2003**, *183*, 31–46. [[CrossRef](#)]
36. Hościło, A.; Lewandowska, A. Mapping forest type and tree species on a regional scale using multi-temporal sentinel-2 data. *Remote Sens.* **2019**, *11*. [[CrossRef](#)]
37. Pouteau, R.; Gillespie, T.W.; Birnbaum, P. Predicting tropical tree species richness from normalized difference vegetation index time series: The devil is perhaps not in the detail. *Remote Sens.* **2018**, *10*, 698. [[CrossRef](#)]
38. Mutanga, O.; Skidmore, A.K. Red edge shift and biochemical content in grass canopies. *ISPRS J. Photogramm. Remote Sens.* **2007**, *62*, 34–42. [[CrossRef](#)]
39. Wessel, M.; Brandmeier, M.; Tiede, D. Evaluation of different machine learning algorithms for scalable classification of tree types and tree species based on sentinel-2 data. *Remote Sens.* **2018**, *10*, 1419. [[CrossRef](#)]
40. Immitzer, M.; Atzberger, C.; Koukal, T. Tree species classification with random forest using very high spatial resolution 8-BandWorldView-2 satellite data. *Remote Sens.* **2012**, *4*, 2661–2693. [[CrossRef](#)]
41. Van Passel, J.; De Keersmaecker, W.; Somers, B. Monitoring woody cover dynamics in tropical dry forest ecosystems using sentinel-2 satellite imagery. *Remote Sens.* **2020**, *12*, 1276. [[CrossRef](#)]
42. Reiche, J.; Verhoeven, R.; Verbesselt, J.; Hamunyela, E.; Wielaard, N.; Herold, M. Characterizing tropical forest cover loss using dense sentinel-1 data and active fire alerts. *Remote Sens.* **2018**, *10*, 777. [[CrossRef](#)]
43. Hirschmugl, M.; Deutscher, J.; Sobe, C.; Bouvet, A.; Mermoz, S.; Schardt, M. Use of SAR and optical time series for tropical forest disturbance mapping. *Remote Sens.* **2020**, *12*, 727. [[CrossRef](#)]



© 2020 by the authors. Licensee MDPI, Basel, Switzerland. This article is an open access article distributed under the terms and conditions of the Creative Commons Attribution (CC BY) license (<http://creativecommons.org/licenses/by/4.0/>).